Transcriptomic and Proteomic Analysis of a 14-3-3 Gene-Deficient Yeast†

Tohru Ichimura,*,‡ Hiroyuki Kubota,§ Takeshi Goma,‡ Noboru Mizushima,# Yoshinori Ohsumi,# Maki Iwago,‡ Kazue Kakiuchi,‡ Hossain Uddin Shekhar,‡ Takashi Shinkawa,‡ Masato Taoka,‡ Takashi Ito,§,|| and Toshiaki Isobe‡,⊥

Department of Chemistry, Graduate School of Science, Tokyo Metropolitan University, Hachioji-shi, Tokyo 192-0397, Japan, Division of Genome Biology, Cancer Research Institute, Kanazawa University, 13-1 Takaramachi, Kanazawa 920-0934, Japan, Department of Cell Biology, National Institute for Basic Biology, 38 Nishigonaka, Myodaijicho, Okazaki 444-8585, Japan, Department of Computational Biology, Graduate School of Frontier Sciences, University of Tokyo, 5-1-5 Kashiwanoha, Kashiwa 277-8561, Japan, and Integrated Proteomics System Project, Pioneer Research on Genome the Frontier, MEXT, c/o Department of Chemistry, Graduate School of Science, Tokyo Metropolitan University, Hachioji-shi, Tokyo 192-0397, Japan

Received August 8, 2003; Revised Manuscript Received March 9, 2004

ABSTRACT: *BMH1* and *BMH2* encode *Saccharomyces cerevisiae* 14-3-3 homologues whose exact functions have remained unclear. The present work compares the transcriptomic and proteomic profiles of the wild type and a *BMH1/2*-deficient *S. cerevisiae* mutant (*bmh*Δ) using DNA microarrays and two-dimensional polyacrylamide gel electrophoresis. It is reported here that, although the global patterns of gene and protein expression are very similar between the two types of yeast cells, a subset of genes and proteins (a total of 220 genes) is significantly induced or reduced in the absence of Bmh1/2p. These genes include approximately 60 elements that could be linked to the reported phenotypes of the *bmh*Δ mutant (e.g., accumulation of glycogen and hypersensitivity to environmental stress) and/or could be the potential downstream targets of interacting partners of Bmh1/2p such as Msn2p and Rtg3p. Importantly, >30% of the identified genes (71 genes) were found to be associated with carbon (C) and nitrogen (N) metabolism and transport, thereby suggesting that Bmh1/2p may play a major role in the regulation of C/N-responsive cellular processes. This study presents the first comprehensive overview of the genes and proteins that are affected by the depletion of Bmh1/2p and extends the scope of knowledge of the regulatory roles of Bmh1/2p in *S. cerevisiae*.

The 14-3-3 proteins comprise a family of acidic, dimeric proteins with subunit molecular masses of ∼30 kDa (*1*). This protein family is highly conserved among eukaryotes, and, in most cases, multiple isoforms are found within a single species, for example, at least 9 in man and 10 in *Arabidopsis*. The 14-3-3 family binds to a variety of proteins in intracellular signaling pathways and participates in the regulation of cell proliferation, differentiation, and function (for reviews, see refs *2* and *3*).

In the yeast *Sacchromyces cerevisiae*, two proteins encoded by the *BMH1* and *BMH2* genes are members of the 14-3-3 family (*4*−*6*). They are ∼60% identical to the mammalian ϵ isoform in their amino acid sequences, and their functions can be complemented with at least one human and four plant 14-3-3 isoforms (*5*, *7*). Previous studies have revealed that Bmh1p and Bmh2p are involved in regulation of the signaling pathway from GTPase Ras via protein kinase A (*6*), the receptor-mediated endocytosis of clathrin-coated vesicles (*6*), and the Ras-MAPK[1] cascade that functions during pseudohyphal development (*8*). It has also been demonstrated recently that the Bmh proteins positively regulate the target of rapamycin (Tor)-mediated cell signaling (*9*). There are currently at least 15 proteins that have been identified as physical and/or genetical interaction partners of Bmh1p and/or Bmh2p, such as those in *TOR* signaling pathways and in cell cycle checkpoint machineries (for a review, see ref *10*). On the basis of these findings, it has been proposed that, like the higher eukaryote 14-3-3 proteins, Bmh proteins are key regulators in a variety of cell signaling pathways in *S. cerevisiae* (for a review, see ref *10*).

However, the overall roles of Bmh1/2p in complex cell signaling pathways are poorly understood at present. To elucidate the roles of Bmh1/2p in yeast cells, a *BMH1/2*-deficient yeast model (*bmh*Δ) was developed with *S. cerevisiae* Σ1278b strains (*8*). The Σ1278b strains, which are mainly used in European laboratories, are known to have unique genetic features for nitrogen metabolism and morphological characteristics for diploid pseudohyphal development and haploid invasive growth (*8*, *11*, *12*). Phenotype studies have revealed that, compared with wild-type Σ1278b cells (e.g., RRY1045 and RRY3; see ref *8*), *bmh*Δ mutants (e.g., RRY1257 and RRY1216; see ref *8*) exhibit increased sensitivity to environmental stress such as heat, high osmolarity, and caffeine. It has also been demonstrated that the

† This work was supported in part by Grants-in-Aid for Scientific Research and by Grants for the Integrated Proteomics System Project, Pioneer Research on Genome the Frontier from MEXT of Japan.

* Author to whom correspondence should be addressed (telephone 81-426-77-2543; fax 81-426-77-2525; e-mail ichimura@mail.comp.metro-u.ac.jp).

‡ Tokyo Metropolitan University.

§ Kanazawa University.

National Institute for Basic Biology.

|| University of Tokyo.

⊥ MEXT.

[1] Abbreviations: MAPK, mitogen-activated protein kinase; MAPKKK, MAPK kinase kinase; MT, mitochondria; ORF, open reading frame; SD, synthetic dropout; SD_{LR}, standard deviation ln(ratio); 2D-PAGE, two-dimensional polyacrylamide gel electrophoresis.

10.1021/bi035421i CCC: $27.50
Published on Web 04/28/2004

mutant cells do not grow on galactose, accumulate high amounts of glycogen, are unable to sporulate, and exhibit abnormal budding patterns (*8*). These phenotypes suggest that Bmh1/2p could play regulatory roles in more diverse pysiological processes than their predicted roles in the reported signal transduction pathways.

To investigate the potential roles of Bmh1/2p in yeast cells, we compared the transcriptional profiles of the wild type and a *bmh*Δ mutant by using high-density DNA filters (microarrays). As a complementary approach, we employed two-dimensional electrophoresis coupled with mass spectrometry to determine the levels of proteome. In this paper we report 220 genes whose expression is significantly affected in the absence of Bmh1/2p.

MATERIALS AND METHODS

Strains and Culture Conditions. The wild-type strain RRY3 (a *ura3-52 his3*) and the *bmh*Δ mutant strain RRY1216 (a *bmh1::HIS3 bmh2::HIS3 ura3-52 his3 leu2*), both of which are congenic as the Σ1278b genetic background, were provided by Dr. G. Fink (Massachusetts Institute of Technology). To construct the *HIS3*-complemented RRY3 and the *LEU2*-complemented RRY1216, two pairs of PCR primers [5′-GGG AAG TCA TAA CAC AGT CC-3′ and 5′-CGG AAT ACC ACT TGC CAC C-3′ (for *HIS3*); 5′-GAA AGG TGA GAG CGC CGG AAC-3′ and 5′-CTT ATC ACG TTG AGC CAT TAG-3′ (for *LEU2*)] were synthesized, each of which had been designed to contain ∼20 base pairs of homology with the flanking regions of the *HIS3* and *LEU2* genes. PCR was performed using genomic DNA from the strain S288C as a template, and the PCR products were used to transform RRY3 and RRY1216. Transformants were selected for histidine or leucine prototrophy. Cultures were performed at 30 °C in a 1-L Erlenmeyer flask containing 300 mL of synthetic dropout (SD) medium (0.67% yeast nitrogen base without amino acids, 2% glucose), supplemented with required amino acids. Cultures were shaken at 200 rpm until growth to the mid-log-phase (OD_{600} of ∼1.0).

DNA Microarrays. The cells in 300-mL portions of the cultures (∼5×10^8/mL) were collected by centrifugation and washed twice with 10 mM Tris (pH 7.5). After the cells had been collected again, total cellular RNAs were isolated using a simplified hot phenol method (*13*). Total RNAs were used for first-strand cDNA synthesis in the presence of Cy3- or Cy5-labeled dUTP (Amersham Pharmacia Biotech). The purified fluorescence-labeled cDNAs were then hybridized to 6118 yeast cDNA microarrays (DNA Chip Research Institute) at 65 °C overnight under conditions of 5× SSC and 0.5% SDS. Fluorescent images of hybridized microarrays were obtained using a GenePix 4000A microarray scanner (Axon Instruments Inc.). The signal intensity of each spot was determined with Gene Pix 3.0 software (Axon Instruments Inc.). The values were converted from log space, and fluorescence ratios (e.g., Cy5/Cy3) were determined. The fluorescence ratios were averaged with data from two independent experiments.

Protein Extraction and Two-Dimensional Gel Electrophoresis. Cells in 600-mL portions of cultures were collected, washed twice with 10 mM Tris (pH 7.5), and then resuspended in 30 mL of the same buffer containing a cocktail of protease inhibitors (5 μg/mL each of pepstatin, aprotinin, and leupeptin and 1 mg/mL benzamidin). After the cells had been pelleted again, soluble proteins were extracted with a Heuser-type cryopress freezing machine (Microtec Co., Ltd.). Yeast mitochondria were prepared as described previously (*14*). Mitochondrial proteins were extracted in breaking buffer comprising 1% Triton X-100, 10 mM Tris (pH 7.4), 0.5 mM EDTA, 2 mM PMSF, 5 μg/mL pepstatin, 5 μg/mL aprotinin, 5 μg/mL leupeptin, and 1 mg/mL benzamidin. Protein concentrations were determined according to the Bradford method with bovine serum albumin as the standard. Two-dimensional electrophoresis was carried out using an immobilized pH gradient gel (IPG gel; pH3−10NL, 180 mm; Amersham Pharmacia Biotech) as described previously (*15*). Silver staining was performed without glutaraldehyde as described (*15*). Quantitation of spots and comparative analysis were performed with Melanie II software (Bio-Rad).

Mass Spectrometry. Protein spots were excised from the 2D gels and in-gel digested with trypsin, and the resulting peptides were analyzed with the direct nanoflow LC-MS/MS system, equipped with an electrospray interface reversed-phase column, a nanoflow gradient device, a high-resolution Q-TOF hybrid MS (Q-TOF2, Micromass), and an automated data analysis system (*16*). The method used was described previously (*17*). All of the MS/MS spectra were searched against the nonredundant protein sequence database maintained at the National Center for Biotechnology Information to identify proteins with the Mascot program (Matrixscience). The MS/MS signal assignments were also confirmed manually.

Assay for Autophagy. For microscopic analysis of autophagic body accumulation, cells were starved in SD (−N) medium (0.17% yeast nitrogen base without amino acids and ammonium sulfate, 2% glucose) for 5 h in the presence of 1 mM PMSF to inhibit degradation of autophagic bodies in the vacuoles. Accumulation of autophagic bodies was detected under a light microscope with Nomarsky optics as described (*18*). For Western blotting of yeast cell lysates, cells were grown to 1 OD_{600} unit/mL and then starved for 3 h in SD (−N) medium to induce autophagy. Ten OD_{600} units of cells were harvested by centrifugation and directly resuspended in 100 μL of 0.2 M NaOH containing 0.5% 2-mercaptoethanol. The cells were kept for 15 min on ice, mixed with 1 mL of cold acetone, and then incubated for 30 min at −20 °C. After centrifugation at 15000*g* for 5 min, the pellets were resuspended in 200 mL of SDS sample buffer and boiled for 5 min. The cell lysates were subjected to SDS−PAGE and immunoblotting with anti-API antibodies.

RESULTS AND DISCUSSION

*mRNA and Protein Expression Profiles of the bmh*Δ *Mutant.* To identify the genes whose expression is affected by the deletion of *BMH1/2* genes, we compared the transcriptomic profiles of the wild-type strain, RRY3, and the *bmh*Δ mutant, RRY1216, both of which are Σ1278b-derived haploid cells that have been employed in studies on pheromone-induced growth arrest, induction of FUS1-LacZ transcription, formation of mating projections, and diploid formation (*8*). The RRY3 and RRY1216 strains were cultured in SD medium supplemented with the required amino acids,

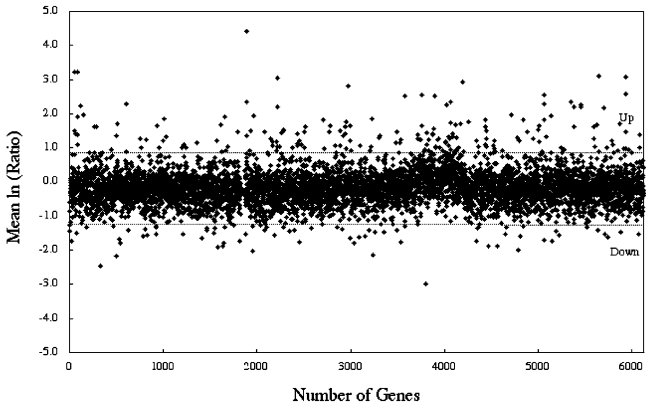

FIGURE 1: Microarray analysis of RRY3 (*wt*) and RRY1216 (*bmh*Δ). Total cellular RNAs were prepared from the RRY3 and RRY1216 strains and used for Cy-3 and Cy-5 labeling, respectively. The mean signal intensity ratios of the mutant to wild-type mRNA levels were obtained from two independent replicate experiments for each gene (see Materials and Methods). The fluorescence ratios are plotted logarithmically. The averaged value of total signal intensities and the standard derivation (SD_{LR}) are −0.16 and 0.52, respectively ($n = 6118$). The statistical data points (0.88 and −1.20, corresponding to $-0.16 \pm 2\text{-}SD_{LR}$, see the text) are indicated by the dashed lines.

and total cellular RNAs were isolated at the middle logarithmic growth phase (OD_{600} of ∼1.0). Cy3- or Cy5-labeled cDNAs were prepared using the purified RNAs as templates and then hybridized with the DNA filters containing 6118 ORFs, which covered >95% of the total ORFs of the yeast (S288C) genome (see Materials and Methods). Figure 1 illustrates the relative transcriptional responses of the mutant to the wild-type mRNA levels, which were expressed as mean natural log-transformed fluorescence ratios of two independent experiments. The fluorescence values of most of the genes were highly reproducible between the two independent analyses (data not shown; see Table S1 in the Supporting Information, Experiments 1 and 2). On the basis of a statistical threshold of $2\text{-}SD_{LR}$ corresponding to >2.4-fold changes, a total of 265 genes were extracted as the genes whose expression was significantly affected in the RRY1216 mutant (Table S1 in the Supporting Information).

The RRY1216 genome carries the *leu2*-null mutation in addition to the deletion of *BMH1/2* genes, whereas the RRY3 genome has the *his3*-null mutation (*8*; also see Materials and Methods). We examined therefore whether the difference in these auxotrophic marker genes could make a major contribution to our microarray data, by comparing the ratios of the RRY1216 to RRY3 mRNA levels with those of the *LEU2*-complemented RRY1216 to *HIS3*-complemented RRY3 mRNA levels. The result showed a linear correlation between the two samples (correlation coefficient = 0.817; Figure 2), suggesting that the observed difference in the expression profiles was primarily caused by the deletion of *BMH1/2* genes. However, it was found that the mRNA levels of 60 of the 265 genes became below the levels of our strict criterion of $2.0\text{-}SD_{LR}$ differences in the complementation experiments (see Figure 2), suggesting that the expression levels of these genes might be affected not only by the deletion of *bmh* genes but also by the mutation of *leu2* and *his3* genes. Thus, we removed these 60 genes from the genes for further characterization in order to minimize the influence of *leu2* and *his3* mutation (shown by asterisks in Table S1).

To determine the effect of the deletion of *BMH1/2* genes at the proteome level, we compared the 2D patterns of proteins expressed in the RRY3 and RRY1216 strains. A water-soluble fraction was prepared from each strain and analyzed by 2D-PAGE and silver staining (see Materials and Methods). Because 14-3-3 proteins were also reported to be present in plant mitochondria (MT) (*19*), MT proteins were prepared, extracted with Triton X-100, and analyzed according to a similar procedure. Comparative 2D gel analysis indicated that, among the 600−1000 spots visualized on the 2D gels, 20 spots for the soluble fraction and 15 for the MT

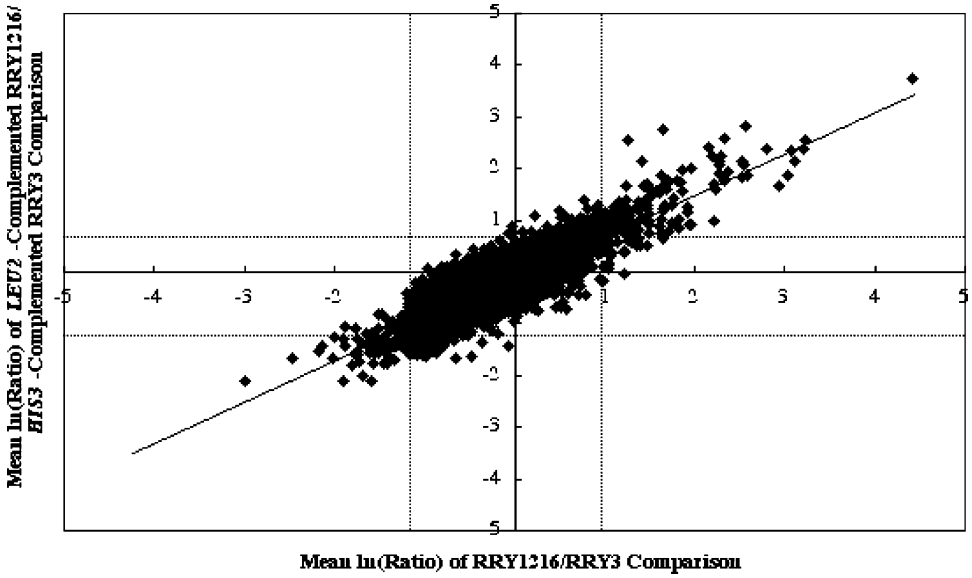

FIGURE 2: Scatter plot of the gene expression ratios (ln scale) in the comparison between RRY1216 and RRY3 (horizontal axis) and between *LEU*2-complemented RRY1216 and *HIS3*-complemented RRY3 (vertical axis). The ratios of the RRY1216 to RRY3 mRNA levels and the ratios of the *LEU*2-complemented RRY1216 to *HIS3*-complemented RRY3 mRNA levels were both obtained from two independent replicate experiments and were transformed to ln(ratios). The transformed RRY1216/RRY3 ratios were plotted against the transformed *LEU*2-complemented RRY1216/*HIS3*-complemented RRY3 ratios. The straight line was drawn by the method of least squares. The dashed lines indicate the statistical data points of $2\text{-}SD_{LR}$ threshold (0.88 and −1.20 for RRY1216/RRY3 comparison; 0.72 and −1.20 for *LEU*2-complemented RRY1216/*HIS3*-complemented RRY3 comparison) required for significance of an expression change.

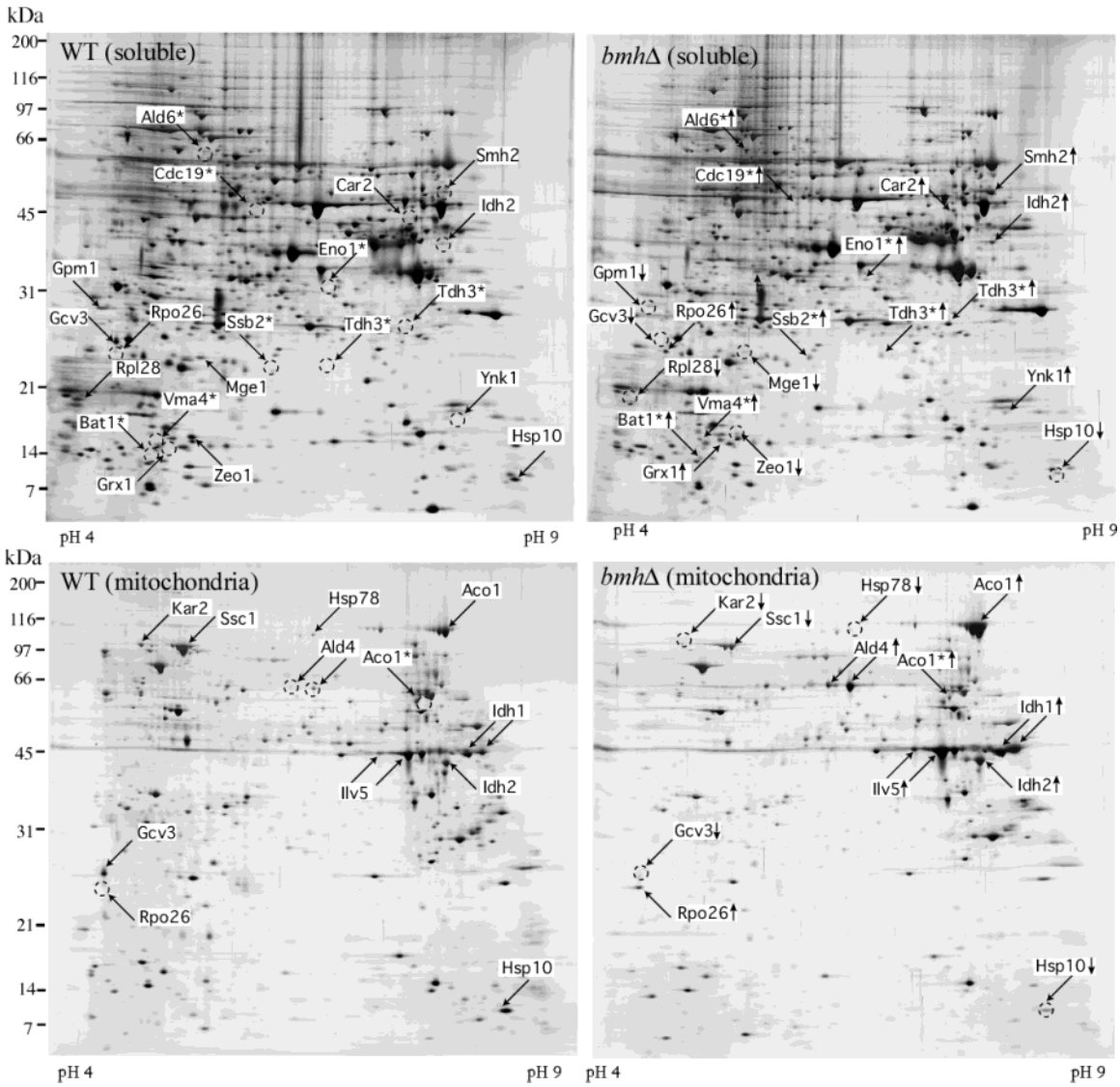

FIGURE 3: 2D-PAGE profiles of RRY3 (*wt*) and RRY1216 (*bmh*Δ). Soluble proteins (500 μg each, upper panels) and mitochondrial proteins (300 μg each, lower panels) were prepared from each of the RRY3 and RRY1216 strains and then analyzed by 2D-PAGE and silver staining. Protein spots with different expression profiles (2.5-fold difference) in the two strains are indicated by arrows and names. The approximate p*I* is indicated along the horizontal axis. The approximate positions of the SDS−PAGE molecular mass standards are indicated in kilodaltons along the vertical axis.

fraction (total 35 spots) showed reproducible changes in expression levels (2.5-fold higher or lower) in triplicate experiments (Figure 3). These spots were excised from the 2D gels and in-gel digested with trypsin, and the resulting peptides were analyzed by direct nanoflow LC-coupled electrospray tandem mass spectrometry to identify the corresponding proteins (see Materials and Methods).

By this procedure, we identified 18 unique proteins (Table S2 in the Supporting Information). The remaining 17 spots allowed repetitive assignments of a single protein or were fragments that resulted from proteolysis of abundant proteins such as Tdh3p and Eno1p (Figure 3, indicated by an asterisk), probably due to posttranslational modifications in the yeast cells or artificial cleavage during our experimental procedures.

Twelve genes (*ALD4*, *CAR2*, *KAR2*, *IDH2*, *IDH1*, *ILV5*, *ACO1*, *SSC1*, *HSP10*, *RPL12*, *MGE1*, and *HSP78*) were identified as ones affected by the deletion of *BMH1/2* genes at both mRNA and protein levels, whereas the difference in the mRNA levels of the latter nine genes (>1.3-SD_{LR}) was just below the statistical threshold of our criteria (Table S2 in the Supporting Information). This suggests that the observed alterations in the expression level of these gene products might be controlled at the transcription level. In contrast, a less significant change in the mRNA levels (<0.6-SD_{LR} difference) was observed for five genes (*RPO26*, *GRX1*, *YNK1*, *GPM1*, and *GCV3*) identified on the proteomic analysis. We also note that the gene *RPO26* was up-regulated at the mRNA level and down-regulated at the protein level (Table S2 in the Supporting Information). These observations suggest that posttranslational regulatory processes may also contribute to the observed differences.

Functional Classification of the Genes Affected by the bmh Null Mutation. The genes and proteins identified on transcriptome and proteome analyses (total of 220 genes) were searched against the yeast proteome database YPD and the *Saccharomyces* genome database SGD and were sorted according to their annotated cellular roles (Figure 4). The largest group of genes that was affected by the *bmh* null mutation comprises 85 genes (or 39% of the total identified

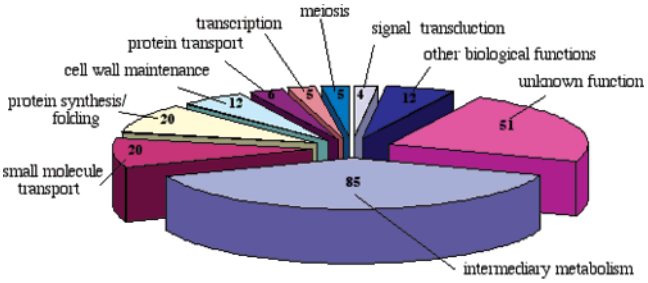

FIGURE 4: Functional class analysis of the identified gene products. Each of the identified gene products was functionally classified according to the yeast proteome database YPD and the *Saccharomyces* genome database SGD. After functional class assessment of each gene product, the total number and percentage of the gene products in each class were determined.

genes) that encode for the enzymes involved in intermediary metabolism, notably those in the TCA cycle (*ACO1*, *CIT1*, *CIT3*, *FUM1*, *IDH1*, *IDH2*, and *SDH2*) and in carbohydrate, amino acid, and lipid metabolism (Table S3 in the Supporting Information). The second largest group of genes affected in the *bmh*Δ mutant is composed of a pair of 20 genes (or 9% of the total identified genes) that encode for transporters of amino acids, etc., and for proteins involved in protein synthesis and folding. The cellular roles of other genes include ones concerning cell wall maintenance (12 genes), transcription (6 genes), protein transport (5 genes), meiosis (5 genes), signal transduction (4 genes), and other biological processes (12 genes). Thus, it appears that the *bmh* mutation is associated with the expression of a variety of genes with distinct cellular roles. The remaining 51 genes (or 23% of the identified genes) are ORFs whose functions have not yet been determined.

Characterization of Genes Involved in Carbon- and Nitrogen-Responsive Cellular Processes. The functional classification based on the YPD and SGD databases indicates that many of the genes identified here are ones involved in carbon (glucose) and nitrogen (amino acid) utilization and transport. Indeed, among the 220 genes identified in this study, >30% (total of 71 genes) belong to this category (Table 1). This suggests that one of the major effects of the *bmh* null mutation is associated with the expression of C- or N-responsive genes. In *S. cerevisiae*, at least three kinase pathways are required for the transcription of many C- or N-responsive genes, RAS/cAMP-dependent protein kinase A (encoded by the *TPK* gene) pathway, *SNF1* (sucrose nonfermenting kinase-1) pathway, and *TOR* pathway (*20*−*23*). Interestingly, we found that the expression of at least 29 genes downstream of these pathways was also affected by the deletion of *BMH1/2* genes, *ACO1*, *ACS1*, *ADE4*, *ARG3*, *ARG8*, *ASN1*, *ASN2*, *CAR2*, *CIT1*, *CIT2*, *CTA1*, *ERG13*, *GCV3*, *GDH1*, *GRX1*, *HSP12*, *HSP78*, *IDH1*, *ID2H*, *ILV5*, *JEN1*, *LYS1*, *PMT2*, *POX1*, *PUT1*, *RTN2*, *SDH2*, *SOL4*, and *YNL134C* (also see below). Taken together, these observations suggest strongly that Bmh1/2p play major roles in C- or N-responsive cellular processes, presumably through the regulation of these protein kinase pathways.

*Characterization of Genes Potentially Linked to bmh*Δ *Phenotypes.* Because the *bmh*Δ mutants exhibit several phenotypes including increased sensitivity to environmental stress, accumulation of glycogen, and defects in sporulation (*8*), it was expected that Bmh1/2p essentially affect some genes required for the control of these pathways. Considering the functions of the genes identified in this study, we indeed observed that the functions of at least 31 genes could be linked to the reported phenotypes. These genes are summarized in Table 2. Among them, the two genes reduced in the *bmh*Δ mutant, *ILS1* (isoleucine-tRNA ligase) and *SPF1* (putative Ca^{2+}-transporting ATPase), may be the key molecules for cellular stress responses, because a strain defective in either of these genes exhibits hypersensitivity to oxidation or multiple drugs (*24*, *25*). Likewise, the gene down-regulated in the *bmh*Δ mutant, *PGM1* (phosphoglucomutase), seems to be necessary for glucose utilization (*26*). In addition, genetic evidence indicates that the five other genes, *KAR2*, *HSP10*, *HSP78*, *MGE1*, and *SSC1* (chaperons), play critical roles in cellular stress responses (*27*−*32*). Thus, the reduced expression observed for these eight genes could correlate directly to some of the phenotypes associated with the *bmh* null mutation. However, the transcription of many other genes, including *BAP2* (branched-chain aliphatic amino acid transporter) and *DAK2* (dihydroxyacetone kinase), was found to be increased in the *bmh*Δ mutant (see Table 2). The fact that the expression of some of these genes (e.g., *BAP2* and *DAK2*) increases the resistance of yeast cells to a variety of cellular stresses (*33*, *34*) suggests that they might be regarded as compensating for the reduction in the eight genes mentioned above, but this awaits further investigations.

One of the phenotypes of the *bmh*Δ mutant is abnormal accumulation of glycogen within the cells. Because a similar phenotype was observed for yeast strains defective in autophagy (*35*), a process required for the degradation and recycling of nonessential cellular proteins, we examined whether the *bmh*Δ mutant might have defects in this process by examining the accumulation of autophagic bodies and the processing of aminopeptidase I (*18*). However, both processes appeared to be normal in the mutant (Figure 5), suggesting that a different mechanism(s) might participate in the observed phenotype.

Characterization of Genes Downstream of Interaction Partners of Bmh1/2p. Bmh proteins bind physically or genetically to at least 15 yeast proteins (*10*). We observed that the expression of 19 genes downstream of the three reported interaction partners for them, Rtg3p (transcription factor; *36*), Msn2p (transcription factor; *23*), and Ste20p (MAPKKKK; *8*), were affected in the *bmh*Δ mutant (Table 3). Recent large-scale analyses of yeast protein complexes (*37*, *38*) have identified an additional 15 proteins that bind physically to Bmh1/2p. We also found 4 and 10 genes downstream of Adr1p (transcription factor; *39*) and the Mbf1p/Gcn4p complex (transcription complex; *40*), respectively, both of which are known to bind with Bmh1p (see Table 3). Thus, our data include a total 33 genes that could represent potential downstream targets of the reported interaction partners of Bmh1/2p.

(1) Downstream Genes of Rtg3p. The five genes *ACO1*, *CIT1*, *CIT2*, *IDH1*, and *IDH2* are the Rtg3p-induced primary response genes that encode for enzymes in the TCA cycle, etc. (Table 3). It is believed that the expression of these genes is negatively regulated through the Tor kinase pathway, because their expression can be induced in yeast cells by the addition of rapamycin, a specific inhibitor of Tor kinases (*41*). Our results show that, like the effect of rapamycin, the expression of all five target genes of Rtg3p is induced in *bmh*-deficient cells (see Table 3). This observation supports

Table 1: Carbon- or Nitrogen-Responsive Genes Whose Expression Is Significantly Affected in the *bmh*Δ Mutant

gene	ID	relative expression ratio RRY1216/RRY3[a]	protein	inducer[b]
carbohydrate metabolism (30 genes)				
ACO1	YLR304C	2.6 (P)	aconitate hydratase	HAP1; HAP2; RTG1; RTG2; RTG3
ACS1	YAL054C	25.8 (T)	acetate-CoA ligase	ADR1; CAT8; SNF; ABF1
ADH4	YGL256W	8.9 (T)	alcohol dehydrogenase	ZAP1
ALD4	YOR374W	5.5 (T), 6.2 (P)	aldehyde dehydrogenase	?
CIT1	YNR001C	3.3 (T)	citrate (Si)-synthase	HAP2; HAP3; HAP4; HAP5; RTG1
CIT2	YCR005C	2.5 (T)	citrate (Si)-synthase	RTG1; RTG2; RTG3; CIT1; MDH1
CIT3	YPR001W	13.5 (T)	citrate (Si)-synthase	?
FSP2	YJL221C	2.8 (T)	α-glucosidase	?
FUM1	YPL262W	2.7 (T)	fumarate hydratase	?
GPH1	YPR160W	4.0 (T)	glycogen phosphorylase	HOG1; heat; heat shock
GSY2	YLR258W	3.3 (T)	glycogen (starch) synthase	heat; nitrogen source limitation
ICL1	YER065C	7.0 (T)	isocitrate lyase	SSN6; acetate; ethanol
IDH1	YNL037C	3.5 (P)	isocitrate dehydrogenase (NAD) subunit 1	RTG1
IDH2	YOR136W	8.6 (P)	isocitrate dehydrogenase (NAD) subunit 2	RTG1; RTG2; RTG3
IDP2	YLR174W	3.5(T)	isocitrate dehydrogenase (NADP)	?
MAL12	YGR292W	5.2 (T)	α-glucosidase	?
MAL32	YBR299W	5.7 (T)	α-glucosidase	?
PCD1	YLR151C	2.9 (T)	phosphoric monoester hydrolase	?
SDH2	YLL041C	3.5 (T)	succinate dehydrogenase	HAP2; HAP3; HAP4; HAP5
SOL4	YGR248W	3.1 (T)	possible 6-phosphogluconolactonase	MSN2; MSN4
SUC2	YIL162W	5.9 (T)	*β*-fructofuranosidase	CTI6; MOT3; MTH1; PKC1; RGT2
YAL061W	YAL061W	4.7(T)	oxidoreductase	PDR1-3 mutation; PDR1-6 mutation
YAT2	YER024w	5.7 (T)	carnitine *O*-acetyltransferase	?
YJL216C	YJL216C	2.6 (T)	α-glucosidase	?
YLR345W	YLR345W	2.5 (T)	fructose-2,6-bisphosphate 2-phosphatase	?
YOL157C	YOL157C	2.8 (T)	α-glucosidase	?
YPL088W	YPL088W	2.9 (T)	alcohol dehydrogenase	PDR1; YRR1
GPM1	YKL152C	0.20 (P)	phosphoglycerate mutase	GCR1
PGM1	YKL127W	0.24 (T)	phosphoglucomutase	STE12; GCR1; GCR2; α factor
PMI40	YER003C	0.15 (T)	mannose-6-phosphate isomerase	PAF1
amino acid metabolism (28 genes)				
ACH1	YBL015W	9.4 (T)	acetyl-CoA hydrolase	stationary phase
ARO9	YHR137W	6.3 (T)	aromatic amino acid aminotransferase	ARO80; methylmethanesulfonate
BIO2	YGR286C	4.6 (T)	biotin synthase	?
BIO3	YNR058W	10.4 (T)	DAPA aminotransferase	?
BIO4	YNR057C	6.6 (T)	dethiobiotin synthase	?
CAR2	YLR438W	18.7 (T), 6.0(P)	ornithine aminotransferase	STE12; STE7; TEC1; DAL81; DAL82
ICL2	YPR006C	4.3 (T)	2-methylisocitrate lyase	ethanol; threonine
ILV5	YLR355C	3.0 (P)	ketol-acid reductoisomerase	GCN4; LEU3
MET2	YNL277W	3.6 (T)	homoserine *O*-acetyltransferase	MET4; cadmium
MET3	YJR010W	6.5 (T)	sulfate adenylyltransferase	MET3p; SRP1; LIN1
MET10	YFR030W	4.6 (T)	sulfite reductase (NADPH) subunit	cadmium; methylmethanesulfonate
MET17	YLR303W	10.4 (T)	*O*-acetylhomoserine aminocarboxy-propyltransferase	MET4; cadmium
MHT1	YLL062C	5.3 (T)	homocysteine *S*-methyltransferase	MET4
PUT1	YLR142W	13.5 (T)	proline dehydrogenase	GAT1; GLN3; PUT3; SNF1
STR3	YGL184C	3.6 (T)	carbon−sulfur lyase	?
ARG1	YOL058W	0.18 (T)	argininosuccinate synthase	?
ARG3	YJL088W	0.20(T)	ornithine carbamoyltransferase	GCN4; methylmethanesulfonate
ARG8	YOL140W	0.21 (T)	acetylornithine transaminase	GCN4; heat
ASN1	YPR145W	0.21 (T)	asparagine synthase	GCN4; HAP2; HAP3; PDR1
ASN2	YGR124W	0.23 (T)	asparagine synthase	GCN4
GCV3	YAL044C	0.09 (P)	glycine cleavage H protein	GCN4; diammonium phosphate
GDH1	YOR375C	0.24 (T)	glutamate dehydrogenase (NADP)	GCN4; HAP2; HAP3; GLN3; ADA2
LYS1	YIR034C	0.19 (T)	saccharopine dehydrogenase (NAD, L-lysine forming)	GCN4; LYS14; 2-aminoadipate semialdehyde
LYS2	YBR115C	0.09 (T)	α-aminoadipate-semialdehyde dehydrogenase large chain	?
LYS4	YDR234W	0.21 (T)	homoaconitate hydratase	?
LYS9	YNR050C	0.18 (T)	saccharopine dehydrogenase (NADP, L-glutamate-forming)	LYS14; PDR1
SAH1	YER043C	0.16 (T)	*S*-adenosylhomocysteinase	BAS1;PHO2
YFR055W	YFR055W	0.13 (T)	cystathionine *β*-lyase	RPD3; methylmethanesulfonate

Table 1 (Continued)

gene	ID	relative expression ratio RRY1216/RRY3[a]	protein	inducer[b]
carbon and nitrogen transport (13 genes)				
ADY2	YCR010C	10.3 (T)	ammonium transporter	acid-to-alkali phase transition
ATO3	YDR384C	3.2 (T)	ammonium transporter	acid-to-alkali phase transition
BAP2	YBR068C	5.1 (T)	branched-chain aliphatic amino acid transporter	LEU2; PTR3; SSY1; STP1; STP2
CAT2	YML042W	5.9 (T)	carnitine *O*-acetyltransferase	OAF1; PIP2; heat; oleic acid
CRC1	YOR100C	10.7 (T)	carnitine/acyl carnitine carrier	OAF1; PIP2; diauxic shift; heat
JEN1	YKL217W	12.7 (T)	pyruvate and lactate symporter	HAP2; HAP3; CAT8; SNF1
MMP1	YLL061W	12.9 (T)	*S*-methylmethionine permease	?
SFC1	YJR095W	4.0 (T)	succinate:fumarate antiporter	acetate; diauxic shift; ethanol
YLL055W	YLL055W	3.4 (T)	transporter	?
AGP1	YCL025C	0.16 (T)	aromatic amino acid transporter	PTR3; SSY1; isoleucine; leucine
CTP1	YBR291C	0.12(T)	citrate transport protein	LYS14
HNM1	YGL077C	0.29 (T)	choline permease	INO2; INO4
SNF3	YDL195W	0.28 (T)	high-affinity glucose sensor	?

[a] Values were obtained from transcriptome (T) and/or proteome (P) analysis. [b] Inducer represents effectors that cause an increase in the transcription of the gene encoding the protein. The effectors are available in the YPD database.

Table 2: Genes Potentially Linked to *bmh* Phenotypes, As Revealed by DNA Microaray and Proteome Analysis

gene	ID	relative expression ratio RRY1216/RRY3	protein
cell stress (25 genes)			
BAP2	YBR068C	5.1 (T)	branched-chain aliphatic amino acid transporter
CAT2	YML042W	5.9 (T)	carnitine *O*-acetyltransferase
CTA1	YDR256C	3.0 (T)	catalase
DAK2	YFL053W	83.3 (T)	dihydroxyacetone kinase
DDR2	YOL052C-A	7.2 (T)	heat shock protein
GRX1	YCL035C	7.6 (P)	protein disulfide oxidoreductase
GUT2	YIL155C	5.1 (T)	glycerol-3-phosphate dehydrogenase
HSP12	YFL014W	5.0 (T)	heat shock protein
IDP2	YLR174W	3.5 (T)	isocitrate dehydrogenase (NADP)
NCE103	YNL036W	7.1 (T)	?
NDE2	YDL085W	3.5 (T)	NADH dehydrogenase
PDE1	YGL248W	3.5 (T)	cAMP-specific phosphodiesterase
SNO1	YMR095C	5.1 (T)	putative pyridoxine (vitamin B6) biosynthetic enzyme
SNZ1	YMR096W	6.2 (T)	?
SNZ2	YNL333W	5.0 (T)	putative pyridoxine (vitamin B6) biosynthetic enzyme
XBP1	YIL101C	4.5 (T)	stress-induced transcriptional repressor
YGP1	YNL160W	6.2 (T)	?
YPS6	YIR039C	5.4 (T)	aspartic-type endopeptidase
HSP10	YLL026W	0.33 (P)	heat shock protein
HSP78	YDR258C	0.13 (P)	heat shock protein
ILS1	YBL076C	0.27 (T)	isoleucine-tRNA ligase
KAR2	YJL034W	0.17 (T), 0.20 (P)	heat shock protein
MGE1	YOR232W	0.15 (P)	mitochondrial matrix protein import
SPF1	YEL031W	0.23 (T)	putative Ca^{2+}-transporting ATPase
SSC1	YJR045C	0.34 (P)	heat shock protein
glycogen storage (3 genes)			
GPH1	YPR160W	4.0 (T)	glycogen phosphorylase
GSY2	YLR258W	3.3 (T)	glycogen (starch) synthase
PGM1	YKL127W	0.24 (T)	phosphoglucomutase
sporulation (3 genes)			
ADY2	YCR010C	10.3 (T)	ammonium transporter
ATO3	YDR384C	3.2 (T)	ammonium transporter
ZIP2	YGL249W	2.6 (T)	protein involved in meiotic recombination, chromosome synapsis, and synaptonemal complex formation

the previous proposal (*9*, *42*) that Bmh1/2p may be positive regulators of rapamycin-sensitive cell signaling and suggests strongly that the Tor−Rtg3p pathway is a physiological target of Bmh1/2p in yeast cells.

(2) Downstream Genes of Msn2p, Mbf1p/Gcn4p, or Adr1p. The seven genes *GRX1*, *HSP12*, *MSC1*, *RTN2*, *SOL4*, *HSP78*, and *YNL134C*, and the four genes *ACS1*, *CTA1*, *POT1*, and *POX1* are Msn2p- and Adr1p-induced genes, respectively, that encode for the proteins in cellular stress responses or enzymes involved in acetyl-CoA synthesis, etc. (see Table 3). It is also known that the expression of these genes is negatively controlled through the Tpk- and/or Tor-signaling pathways (*23*, *43*) and the Tpk-signaling pathway (*39*), respectively. On the other hand, the 10 genes *ILV5*, *ADE4*, *ARG3*, *ARG8*, *ASN1*, *ASN2*, *GCV3*, *GDH1*, *LYS1*, and *PMT1* are Mbf1p/Gcn4p-induced genes whose expression is positively regulated through the Tpk- or Tor-signaling pathway (*44*, *45*). Our data show that many or all of these

Table 3: Downstream Genes of Reported Interaction Partners of Bmh1/2p Whose Expression Is Significantly Affected in the *bmh*Δ Mutant

gene	ID	relative expression ratio RRY1216/RRY3	protein
Rtg3p pathways (5 genes)			
ACO1	YLR304C	2.6 (P)	aconitate hydratase
CIT1	YNR001C	3.3 (T)	citrate (Si)-synthase
CIT2	YCR005C	2.5 (T)	citrate (Si)-synthase
IDH1	YNL037C	3.5 (P)	isocitrate dehydrogenase (NAD) subunit 1
IDH2	YOR136W	8.6 (P)	isocitrate dehydrogenase (NAD) subunit 2
Msn2p pathways (7 genes)			
GRX1	YCL035C	7.6 (P)	protein disulfide oxidoreductase
HSP12	YFL014W	5.0 (T)	heat shock protein
MSC1	YML128C	3.4 (T)	?
RTN2	YDL204W	5.2 (T)	?
SOL4	YGR248W	3.1 (T)	possible 6-phosphogluconolactonase
HSP78	YDR258C	0.13 (P)	heat shock protein
YNL134C	YNL134C	0.21 (T)	alcohol dehydrogenase
MAPK pathways (7 genes)			
CAR2	YLR438W	18.7 (T), 6.0 (P)	ornithine aminotransferase
PST1	YDR055W	3.8 (T)	putative GPI-anchored protein
RTA1	YGR213C	2.7 (T)	protein involved in 7-aminocholesterol resistance
YLR414C	YLR414C	5.5 (T)	?
YPS1	YLR120C	4.0 (T)	aspartic-type endopeptidase
ERG13	YML126C	0.18 (T)	hydroxymethylglutaryl-CoA synthase
PGM1	YKL127W	0.24 (T)	phosphoglucomutase
Adr1p pathways (4 genes)			
ACS1	YAL054C	25.8 (T)	acetate-CoA ligase
CTA1	YDR256C	3.0 (T)	catalase
POT1	YIL160C	4.2 (T)	acetyl-CoA C-acyltransferase
POX1	YGL205W	3.3 (T)	acyl-CoA oxidase
Mbf1p/Gcn4p pathways (10 genes)			
ILV5	YLR355C	3.0 (P)	ketol-acid reductoisomerase
ADE4	YMR300C	0.22 (T)	amidophosphoribosyltransferase
ARG3	YJL088W	0.20 (T)	ornithine carbamoyltransferase
ARG8	YOL140W	0.21 (T)	acetylornithine transaminase
ASN1	YPR145W	0.21 (T)	asparagine synthase
ASN2	YGR124W	0.23 (T)	asparagine synthase
GCV3	YAL044C	0.09 (P)	glycine cleavage H protein
GDH1	YOR375C	0.24 (T)	glutamate dehydrogenase (NADP)
LYS1	YIR034C	0.19 (T)	saccharopine dehydrogenase (NAD, L-lysine forming)
PMT2	YAL023C	0.18 (T)	dolichyl-phosphate-mannose-protein mannosyltransferase

Msn2p and Adr1p target genes are significantly induced in *bmh*-deficient mutant cells, whereas the majority of the Mbf1p/Gcn4p-target genes are significantly reduced (see Table 3). These observations suggest that Bmh1/2p could act as both positive and negative regulators for the expression of these genes, in concert with the regulatory roles of the Tpk- or Tor-signaling pathway. However, the two genes downstream of Msn2p, *HSP78* and *YNL134C*, were found to be down-regulated, and conversely, the gene downstream of Mbf1p/Gcn4p, *ILV5*, was up-regulated in the *bmh*Δ mutant (see Table 3). This observation suggests that additional regulatory control(s) could also participate in the expression of these genes.

(3) Downstream Genes of Ste20p. The seven genes *CAR2*, *RTA1*, *PST1*, *YLR414C*, *YPS1*, *PGM1*, and *ERG13* are downstream targets of the Ste20p-mediated MAPK pathway (Ste20p-Ste11p-Ste7p-Fus3/Kss1-Ste12p) that encode for the enzymes primarily involved in intermediary metabolism and cell wall maintenance. Our data show that many of these genes are significantly induced in the *bmh*-deficient mutant cells (Table 3). This suggests that Bmh1/2p could negatively regulate the Ste20p pathway. However, as in the case of the Msn2p target genes, some of these genes are also reduced significantly in the *bmh*Δ mutant. Thus, additional factor(s) should be considered to explain the observed gene expression.

Characterization of Genes Downstream of the Ino2p Transcription Factor. A previous study indicated that human 14-3-3 proteins affect a signaling process involving myo-inositol (*46*). In this study, we found that the expression of *INO1*, a gene involved in inositol phosphate metabolism (*47*, *48*), was significantly reduced in the *bmh*Δ mutant (Table S1 in the Supporting Information). It is known that the *INO1* gene is downstream of the basic helix-loop-helix transcription factor Ino2p, which plays an essential role in the transcriptional activation of a number of phospholipid biosynthetic genes (*48*; for a review, see ref *49*). Interestingly, we found that the mRNA levels of four other Ino2p-dependent genes, *FAS2* (fatty-acyl-CoA synthase), *HNM1* (choline permease), *ITR1* (myo-inositol permease), and *PSD1* (phosphatidylserine decarboxylase), were also significantly reduced in the *bmh*-deficient mutant cells (see Table S1 in the Supporting Information). Because the mRNA levels of the *INO*2 gene remained unchanged in the *bmh*Δ mutant (data not shown), these results imply that Bmh1/2p might also function in the pathway for Ino2p-mediated transcriptional control.

Increasing evidence indicates that Bmh1/2p play roles in many fundamental processes of yeast cell viability and

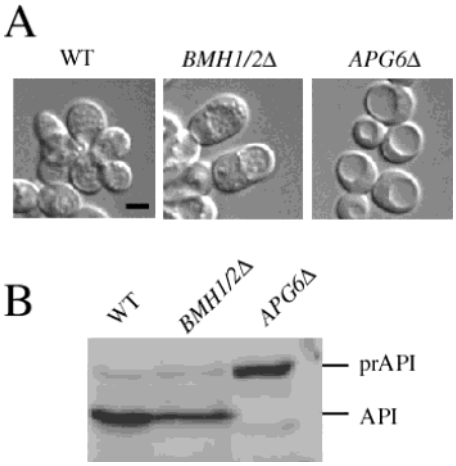

FIGURE 5: Bmh1p and Bmh2p are not essential for autophagy. (A) RRY3 (wt), RRY1216 (*bmh*Δ), and KVY135 (*apg6*Δ) cells were starved in SD (−N) medium containing 1 mM PMSF and then incubated for 5 h. Cells were observed under a light microscopy. Bar = 2 μm. (B) RRY3 (wt), RRY1216 (*bmh*Δ), and KVY135 (*apg6*Δ, REF) cells were starved in SD (−N) medium for 3 h. Aminopeptidase I (API) was detected by Western blotting as described under Materials and Methods. KVY135 cells were used as a positive control for the analysis (*18*).

function. Indeed, although the Σ1278b strains are the only known *S. cerevisiae* strains that do not require the *BMH* genes for survival, several *bmh* mutation phenotypes are also common among other yeast strains. For example, hypersensitivities to stresses, such as heat and rapamycin, were reported for the strain CENPKI13-9D with the temperature-sensitive *bmh2* allele (*36*). In addition, the strain GG582-5C, with a conditional *bmh1 bmh2* double-disruption, exhibits abnormal budding patterns (*5*), which are indistinguishable from those of RRY1216. These observations suggest strongly that the basic functions of Bmh1/2p are highly conserved among *S. cerevisiae*. Our data thus provide important information on the potential roles of Bmh1/2p, not only in Σ1278b but also in other *S. cerevisiae* strains. However, the gene or genes that allow the Σ1278b strains to survive in the absence of Bmh1/2p have not been identified.

In conclusion, we have identified 220 genes whose expression is apparently altered in the *bmh* null mutation. The wide variety of functions of these gene products suggests that Bmh1/2p play roles in diverse kinase-mediated regulatory processes. In addition, these genes include many elements that could account for the reported phenotypes of the *bmh* mutation or could be the downstream targets of known interaction partners of Bmh1/2p. Thus, our data provide notable information on the potential roles of Bmh1/2p in the signal transduction pathways of *S. cerevisiae*. Further studies are needed, however, to clarify the molecular mechanisms by which Bmh1/2p regulate the expression of these downstream genes. Global analysis of proteins associated with Bmh1/2p in Σ1278b cells is presently underway by our research group.

ACKNOWLEDGMENT

We are grateful to Dr. G. Fink (Massachusetts Institute of Technology) for the kind gift of the wild type and *bmh*-deficient yeast cells. We are thankful to Drs. T. Endo and M. Esaki (Nagoya University) for helpful suggestions in the preparation of the yeast mitochondria.

SUPPORTING INFORMATION AVAILABLE

mRNA and protein expression data, as revealed by DNA microarray and proteome analysis. This material is available free of charge via the Internet at http://pubs.acs.org.

REFERENCES

1. Moore, B. W., and Perez, V. J. (1967) Specific acidic proteins of the nervous system, in *Physiological and Biochemical Aspects of Nervous Integration*, pp 343−359, Prentice-Hall, Englewood Cliffs, NJ.
2. Fu, H., Subramanian, R. R., and Masters, S. C. (2000) 14-3-3 proteins, structure, function, and regulation, *Annu. Rev. Pharmacol. Toxicol. 40*, 617−647.
3. Tzvion, G., and Avruch, J. (2002) 14-3-3 proteins: active cofactors in cellular regulation by serine/threonine phosphorylation, *J. Biol. Chem. 277*, 3061−3064.
4. van Heusden, G. P. H., Wenzel, T. J., Lagendijk, E. L., Steensma, H. Y., van den Berg, J. A. (1992) Characterization of the yeast BMH1 gene encoding a putative protein homologous to mammalian protein kinase II activators and protein kinase C inhibitors, *FEBS Lett. 302*, 145−150.
5. van Heusden, G. P. H., Griffiths, D. J. F., Ford, J. C., Chin-A-Woeng, T. F. C., Schrader, P. A. T., Carr, A. M., and Sttensma, H. Y. (1995) The 14-3-3 proteins encoded by the BMH1 and BMH2 genes are essential in the yeast *Saccharomyces cerevisiae* and can be replaced by a plant homologue, *Eur. J. Biochem. 229*, 45−53.
6. Gelperin, D., Weigle, J., Nelson, K., Roseboom, P., Irie, K., Matsumoto, K., and Lemmon, S. (1995) 14-3-3 proteins: potential roles in vesicular transport and Ras signaling in *Saccharomyces cerevisiae*, *Proc. Natl. Acad. Sci. U.S.A. 92*, 11539−11543.
7. van Heusden, G. P. H., van der Zanden, A. L., Ferl, R. J., and Sttensma, H. Y. (1996) Four *Arabidopsis thaliana* 14-3-3 protein isoforms can complement the lethal yeast bmh1 bmh2 double disruption, *FEBS Lett. 391*, 252−256.
8. Roberts, R. L., Mosch, H.-U., and Fink, G. R. (1997) 14-3-3 proteins are essential for RAS/MAPK cascade signaling during pseudohyphal development in *S. cerevisiae*, *Cell 89*, 1055−1065.
9. Bertram, P. G., Zeng, C., Thorson, J., Shaw, A. S., Zheng, X. F. S. (1998) The 14-3-3 proteins positively regulate rapamycin-sensitive signaling, *Curr. Biol. 8*, 1259−1267.
10. van Hemert, M. J., van Heusden, G. P. H., and Steensma, H. Y. (2001) Yeast 14-3-3 proteins, *Yeast 18*, 889−895.
11. Gimeno, C. J., Ljungdahl, P. O., Styles, C. A., and Fink, G. R. (1992) Unipolar cell divisions in the yeast S. cerevisiae lead to filamentous growth: regulation by starvation and RAS, *Cell 68*, 1077−1090.
12. Stanhill, A., Schick, N., and Engelberg, D. (1999) The yeast ras/cyclic AMP pathway induces invasive growth by suppressing the cellular stress response, *Mol. Cell. Biol. 19*, 7529−7538.
13. Schmitt, M. E., Brown, T. A., and Trumpower, B. L. (1990) A rapid and simple method for preparation of RNA from *Saccharomyces cerevisiae*, *Nucleic Acids Res. 18*, 3091−3092.
14. Daum, G., Bohni, P. C., and Schatz, G. (1982) Import of proteins into mitochondria. Cytochrome *b*2 and cytochrome *c* peroxidase are located in the intermembrane space of yeast mitochondria, *J. Biol. Chem. 257*, 13028−13033.
15. Taoka, M., Wakamiya, A., Nakayama, H., and Isobe, T. (2000) Protein profiling of rat cerebella during development, *Electrophoresis 21*, 1872−1879.
16. Natsume, T., Yamauchi, Y., Nakayama, H., Shinkawa, T., Yanagida, M., Takahashi, N., and Isobe, T. (2002) A direct nanoflow liquid chromatography-tandem mass spectrometry system for interaction proteomics, *Anal. Chem. 74*, 4725−4733.
17. Ichimura, T., Wakamiya-Tsuruta, A., Itagaki, C., Taoka, M., Hayano, T., Natsume, T., and Isobe, T. (2002) Phosphorylation-dependent interaction of kinesin light chain 2 and the 14-3-3 protein, *Biochemistry 41*, 5566−5572.
18. Kirisako, T., Ichimura, Y., Okada, H., Kabeya, Y., Mizushima, N., Yoshimori, T., Ohsumi, M., Takao, T., Noda, T., and Ohsumi, Y. (2000) The reversible modification regulates the membrane-binding state of Apg8/Aut7 essential for autophagy and the cytoplasm to vacuole targeting pathway, *J. Cell Biol. 151*, 263−275.

19. Bunney, T. D., van Walraven, H. S., and de Boer, A. H. (2001) 14-3-3 protein is a regulator of the mitochondrial and chloroplast ATP synthase, *Proc. Natl. Acad. Sci. U.S.A. 98*, 4249−4254.
20. Jiang, Y., Davis, C., and Broach, J. R. (1998) Efficient transition to growth on fermentable carbon sources in *Saccharomyces cerevisiae* requires signaling through the Ras pathway, *EMBO J. 17*, 6942−6951.
21. Celenza, J. L., and Carlson, M. (1986) A yeast gene that is essential for release from glucose repression encodes a protein kinase, *Science 233*, 1175−1180.
22. Ludin, K., Jiang, R., and Carlson, M. (1998) Glucose-regulated interaction of a regulatory subunit of protein phosphatase 1 with the Snf1 protein kinase in *Saccharomyces cerevisiae*, *Proc. Natl. Acad. Sci. U.S.A. 95*, 6245−6250.
23. Beck, T., and Hall, M. N. (1999) The TOR signalling pathway controls nuclear localization of nutrient-regulated transcription factors, *Nature 402*, 689−692.
24. Miyamoto, Y., Machida, K., Mizunuma, M., Emoto, Y., Sato, N., Miyahara, K., Hirata, D., Usui, T., Takahashi, H., Osada, H., and Miyakawa, T. (2002) Identification of *Saccharomyces cerevisiae* isoleucyl-tRNA synthetase as a target of the G1-specific inhibitor Reveromycin A, *J. Biol. Chem. 277*, 28810−28814.
25. Tipper, D. J., and Harley, C. A. (2002) Yeast genes controlling responses to topogenic signals in a model transmembrane protein, *Mol. Biol. Cell 13*, 1158−1174.
26. Boles, E., Liebetrau, W., Hofmann, M., and Zimmermann, F. K. (1994) Characterization of the essential yeast gene encoding *N*-acetylglucosamine-phosphate mutase, *Eur. J. Biochem. 221*, 741−747.
27. Normington, K., Kohno, K., Kozutsumi, Y., Gething, M. J., and Sambrook, J. (1989) *S. cerevisiae* encodes an essential protein homologous in sequence and function to mammalian BiP, *Cell 57*, 1223−1236.
28. Rose, M. D., Misra, L. M., and Vogel, J. P. (1989) KAR2, a karyogamy gene, is the yeast homolog of the mammalian BiP/GRP78 gene, *Cell 57*, 1211−1221.
29. Dubaquie, Y., Looser, R., Funfschilling, U., Jeno, P., and Rospert, S. (1998) Identification of in vivo substrates of the yeast mitochondrial chaperonins reveals overlapping but non-identical requirement for hsp60 and hsp10, *EMBO J. 17*, 5868−5876.
30. Rottgers, K., Zufall, N., Guiard, B., and Voos, W. (2002) The ClpB homolog Hsp78 is required for the efficient degradation of proteins in the mitochondrial matrix, *J. Biol. Chem. 277*, 45829−45837.
31. Westermann, B., Prip-Buus, C., Neupert, W., and Schwarz, E. (1995) The role of the GrpE homologue, Mge1p, in mediating protein import and protein folding in mitochondria, *EMBO J. 14*, 3452−3460.
32. Voisine, C., Craig, E. A., Zufall, N., von Ahsen, O., Pfanner, N., and Voos, W. (1999) The protein import motor of mitochondria: unfolding and trapping of preproteins are distinct and separable functions of matrix Hsp70, *Cell 97*, 565−574.
33. Palmer, L. K., Wolfe, D., Keeley, J. L., and Keil, R. L. (2002) Volatile anesthetics affect nutrient availability in yeast, *Genetics 161*, 563−574.
34. Molin, M., Norbeck, J., and Blomberg, A. (2003) Dihydroxyacetone kinases in *Saccharomyces cerevisiae* are involved in detoxification of dihydroxyacetone, *J. Biol. Chem. 278*, 1415−1423.
35. Wilson, W. A., Wang, Z., and Roach, P. J. (2002) Systematic identification of the genes affecting glycogen storage in the yeast *Saccharomyces cerevisiae*: implication of the vacuole as a determinant of glycogen level, *Mol. Cell. Proteomics 1*, 232−242.
36. van Heusden, G. P. H., and Steensma, H. Y. (2001) 14-3-3 Proteins are essential for regulation of RTG3-dependent transcription in *Saccharomyces cerevisiae*, *Yeast 18*, 1479−1491.
37. Gavin, A.-C., Bosche, M., Krause, R., Grandi, P., Marzioch, M., Bauer, A., Schultz, J., Rick, J. M., Michon, A.-M., Cruciat, C.-M., Remor, M., Hofert, C., Schelder, M., Brajenovic, M., Ruffner, H., Merino, A., Klein, K., Hudak, M., Dickson, D., Rudi, T., Gnau, V., Bauch, A., Bastuck, S., Huhse, B., Leutwein, C., Heurtler, M.-A., Copley, R. R., Edelmann, A., Querfurth, E., Rybin, V., Drewes, G., Raida, M., Bouwmeester, T., Bork, P., Seraphin, B., Kuster, B., Neubauer, G., and Superti-Furga, G. (2002) Functional organization of the yeast proteome by systematic analysis of protein complexes, *Nature 415*, 141−147.
38. Ho, Y., Gruhler, A., Heilbut, A., Bader, G. D., Moore, L., Adams, S.-L., Millar, A., Taylor, P., Bennett, K., Boutilier, K., Yang, L., Wolting, C., Donaldson, I., Schandorff, S., Shewnarane, J., Vo, M., Taggart, J., Goudreault, M., Muskat, B., Alfarano, C., Dewar, D., Lin, Z., Michalickova, K., Willems, A. R., Sassi, H., Nielsen, P. A., Rasmussen, K., Andersen, J. R., Johansen, L. E., Hansen, L. H., Jespersen, H., Podtelejnikov, A., Nielsen, E., Crawford, J., Poulsen, V., Sorensen, B. D., Matthiesen, J., Hendrickson, R. C., Gleeson, F., Pawson, T., Moran, M. F., Durocher, D., Mann, M., Hogue, C. W. V., Figeys, D., and Tyers, M. (2002) Systematic identification of protein complexes in *Saccharomyces cerevisiae* by mass spectrometry, *Nature 415*, 180−183.
39. Cherry, J. R., Johnson, T. R., Dollard, C., Shuster, J. R., and Denis, C. L. (1989) Cyclic AMP-dependent protein kinase phosphorylates and inactivates the yeast transcriptional activator ADR1, *Cell 56*, 409−419.
40. Li, F.-Q., Ueda, H., and Hirose, S. (1994) Mediators of activation of fushi tarazu gene transcription by BmFTZ-F1, *Mol. Cell. Biol. 14*, 3013−3021.
41. Komeili, A., Wedaman, K. P., O'Shea, E. K., and Powers, T. (2000) Mechanism of metabolic control. Target of rapamycin signaling links nitrogen quality to the activity of the Rtg1 and Rtg3 transcription factors, *J. Cell Biol. 151*, 863−878.
42. Liu, Z., Sekito, T., Spirek, M., Thornton, J., and Butow, R. A. (2003) Retrograde signaling is regulated by the dynamic interaction between Rtg2p and Mks1p, *Mol. Cell 12*, 401−411.
43. Smith, A., Ward, M. P., and Garrett, S. (1998) Yeast PKA represses Msn2p/Msn4p-dependent gene expression to regulate growth, stress response and glycogen accumulation, *EMBO J. 17*, 3556−3364.
44. Brindle, P., Linke, S., and Montminy, M. (1993) Protein-kinase-A-dependent activator in transcription factor CREB reveals new role for CREM repressors, *Nature 364*, 821−824.
45. Valenzuela, L., Aranda, C., and Gonzalez, A. (2001) TOR modulates GCN4-dependent expression of genes turned on by nitrogen limitation, *J. Bacteriol. 183*, 2331−2334.
46. Nikawa, J. (1994) A cDNA encoding the human transforming growth factor beta receptor suppresses the growth defect of a yeast mutant, *Gene 149*, 367−372.
47. Culbertson, M. R., and Henry, S. A. (1975) Inositol-requiring mutants of *Saccharomyces cerevisiae*, *Genetics 80*, 23−40.
48. Donahue, T., and Henry, S. A. (1981) myo-Inositol-1-phosphate synthase. Characteristics of the enzyme and identification of its structural gene in yeast, *J. Biol. Chem. 256*, 7077−7085.
49. Robinson, K. A., and Lopes, J. M. (2000) Survey and Summary: *Saccharomyces cerevisiae* basic helix-loop-helix proteins regulate diverse biological processes, *Nucleic Acids Res. 28*, 1499−1505.

BI035421I